Journal of Sound and Vibration (1998) **212**(1), 141–164

ACTIVE NOISE CONTROL OF AN INCOHERENT LINE SOURCE

D. Duhamel and P. Sergent

Ecole nationale des ponts et chaussées, CERAM, 6 *et* 8 *Avenue Blaise Pascal, Cité Descartes, Champs-sur-Marne*, 77455 *Marne-La-Vallée Cedex* 2, *France*

(*Received* 22 *November* 1996, *and in final form* 11 *December* 1997)

In this paper the outdoor active noise control of the sound pressure created by an incoherent line source is studied. Such a source is a model for the noise generated by road traffic or by trains and consists of a continuous distribution of uncorrelated point sources. By using this model, the possibility of generating quiet zones for environmental noise is examined. For this purpose the statistical properties of the sound pressure are first studied. Then the efficiency of active control by point sources is calculated as a function of both frequency and position and comparisons are made between finite and infinite length primary sources. Finally, the investigation is extended to the calculation of the pressure crossing an aperture in a rigid plane to simulate the energy entering into a room through an open window. The energy crossing the aperture is calculated with and without control to determine the noise reduction potentially provided by the active control.

1. INTRODUCTION

Active control is now recognized as a powerful tool for reducing low frequency noise for which passive methods are usually inefficient. Several applications have been developed for the control of noise in ducts, in earphones, in cars or aircraft fuselages and in most of these examples important noise reductions have been obtained in the whole space domain, or in a part only. Almost all these applications, however, deal with closed and restricted spaces. There is also a large need for the reduction of environmental noise such as that of road traffic or train noise which lead to important problems not satisfactorily solved in urban areas. This article reports a study of the possibility of using active noise control methods to reduce these types of noise by using an incoherent line as a model for the noise source. The interest in studying incoherent line sources is that they can provide a good model for the noise created by dense road traffic. The point sources correspond to the individual vehicles which emit sound pressures quite independently. It can also be used to model a train if the line has a limited length.

In the domain of active noise control, much less effort has been undertaken to reduce the noise in outdoor application than that in closed domains. Some work, however, can provide interesting insights and allow one to estimate the possibilities of such systems. The simplest problem seems to be the reduction of the sound pressure radiated by a point source in free field by another point source. In this case, Nelson [1] has shown that the total power output can be reduced only if the secondary source is separated from the primary source by a distance which is less than one half wavelength. So for most practical problems of interest such a goal seems unachievable, and one must look for a local control in which the noise is reduced in a limited space domain but with perhaps an increase in

0022–460X/98/160141 + 24 $25.00/0/sv971454

noise elsewhere. Furthermore, in many applications the control of the total sound pressure is not necessary and it is sufficient to create local zones of silence.

The local active noise control in three-dimensional free space of the sound pressure created by a point source was studied by Tokhi [2]. He calculated the extent of the cancellation zone and the stability of the controller according to the geometrical arrangement of the system. Wright and Vuksanovic [3] have made a detailed study of the cancellation zone for active control of the sound pressure created by several primary sources with the same amplitudes and phases and a screen of secondary sources. They showed that the cancellation zone looked like an angular sector with an aperture depending on the frequency and on the geometrical arrangement of the system. Several authors including Ise *et al*. [4], Omoto and Fujiwara [5], Omoto *et al*. [6] and Duhamel [7] have studied active control around noise barriers. In this case the passive efficiency of the barrier at high frequencies could be improved by the effect of active control at low frequencies to provide good noise control over the whole spectrum. The cancellation zone also looks like an angular sector with an opening angle decreasing with the frequency.

In all these active control problems, and even more specifically for outdoor applications, the efficiency of the active systems is limited mainly by two difficulties. The first one is the spectral content of the primary pressure field. It is well known that active control works mainly for low frequencies because the wavelength is large in this case and the cancellation of noise by interference phenomena can have a large spatial extent. Furthermore, the sampling frequency of the digital controller can be chosen to be sufficiently low to be compatible with the possibilities of the electronics. However, if the previous conditions are fulfilled, noise with relatively complex spectra can be controlled with the help of adaptive algorithms such as the LMS.

The second difficulty of active control systems comes from the spatial extent of the primary source. In most active control systems the primary source is rather compact in size. It is, for instance, a fan in duct applications or an engine for cars or airplanes. Our purpose is, however, to study active control for outdoor noise propagations. In these cases the primary source can be very complex. In fact, we will concentrate on road traffic noise modelled as an incoherent line source. This source is made up of an infinite number of uncorrelated three-dimensional point sources positioned along a straight line. This object produces a complex sound field because the pressure at a point comes from different directions corresponding to the different points constituting the line source. The sound pressures coming from these directions are, furthermore, uncorrelated, so we are faced with a sort of diffuse sound field.

Similar problems were studied in the papers of Joseph *et al*. [8, 9], Elliott *et al*. [10], Garcia-Bonito and Elliott [11] and David and Elliott [12] for the case of a reverberant room. They theoretically and experimentally determined the zone of quiet in a pure tone diffuse sound field for active control by a secondary point source and an error microphone placed near the secondary source (at a distance less than a wavelength) or at a larger distance from the source. They found that the zone over which the primary pressure is reduced by more than 10 dB has a diameter of order $\lambda/10$. This problem is different from ours in many aspects. First, it takes place in a closed domain and, second, there is always a unique pair of primary and secondary sources, whereas we have, in our problem, a continuous distribution of uncorrelated primary point sources.

We will here present a specific study of the sound pressure created by an incoherent line source and of the possibility of creating quiet zones by active noise control. We will first give a mathematical model of an incoherent line source with a detailed study of the spatial correlation of the sound pressure which is good information on the complexity of the sound field. Comparisons between time and frequency analyses are investigated. Then we will examine active control in free field, estimating the cancellation zone according to the frequency. The model of an infinite number of discrete point sources located along a straight line is compared to the continuous model and to a line of finite extent which as we will show, will have better properties than the infinite source. However, the cancellation zone that can be obtained by active control has a limited extent. Therefore, only small local zones of quiet can be created in free field. This could be sufficient, however, to reduce the noise entering a room through an open window. To study this problem, the above results will finally be extended to the active control of the noise crossing an aperture in a rigid screen.

2. INCOHERENT LINE SOURCE

An incoherent line source is modelled as a distribution of three-dimensional point sources located on a straight line. One supposes that the sound pressures radiated by two different point sources have no relation so that the sound pressures they emit are fully uncorrelated. This line source has a large spatial extent and generates a much more complex sound field than a standard point source. We will first start our study by giving a precise mathematical model of this source, and then we will study the correlation properties of the sound pressures at two different spatial points for different models of the source: discrete or continuous, finite or infinite.

2.1. MATHEMATICAL MODEL

We consider first the case of harmonic sources with the time dependency $e^{-i\omega t}$ suppressed throughout. The amplitude $\mu(l)$ of the source as function of the abscissa l can be seen as a random process with the cross-correlation function

$$E(\mu(l)\mu^*(l')) = \delta(l - l'), \tag{1}$$

where the asterisk denotes the complex conjugate and E is the expectation. The sources are supposed to have unit strengths and the amplitudes are such that $E(\mu(l)) = 0$. The source has a finite length and is included in the interval $[l_a, l_b]$ in the x_3-axis (see Figure 1 for notations). In free field the pressure of the whole line at a point $\mathbf{x} = (x_1, x_2, x_3)$ is given by

$$p(\mathbf{x}) = \int_{l_a}^{l_b} \frac{e^{ikr}(l)}{4\pi r(l)}\, \mu(l)\, dl, \tag{2}$$

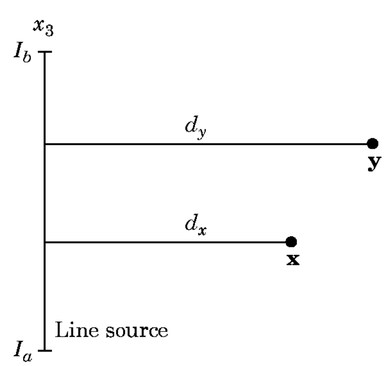

Figure 1. The incoherent line source.

where $r(l)=\sqrt{x_1^2+x_2^2+(x_3-l)^2}$. The pressure $p(\mathbf{x})$ is also a random process. The definition being statistical by nature we will focus our attention on average values obtained by taking the statistical expectation of quantities of interest. For instance, we can calculate the average potential energy in free field which has the expectation

$$e_{free}=\mathrm{E}\left(\frac{|p(\mathbf{x})|^2}{4\rho c^2}\right)=\frac{1}{4\rho c^2}\int_{l_a}^{l_b}\int_{l_a}^{l_b}\frac{\mathrm{e}^{\mathrm{i}kr(l)}}{4\pi r(l)}\frac{\mathrm{e}^{-\mathrm{i}kr(l')}}{4\pi r(l')}\mathrm{E}(\mu(l)\mu^*(l'))\,\mathrm{d}l\,\mathrm{d}l'$$

$$=\frac{1}{4\rho c^2}\int_{l_a}^{l_b}\frac{1}{[4\pi r(l)]^2}\,\mathrm{d}l=\frac{\arctan(l_b/d)-\arctan(l_a/d)}{64\pi^2\rho c^2 d}, \tag{3}$$

where $d=\sqrt{x_1^2+x_2^2}$ is the radial distance from the point $\mathbf{x}$ to the line source. For long sources, this density of potential energy is decreasing as the inverse of the distance to the line source.

2.2. THE SPATIAL CROSS-CORRELATION FUNCTION

The complexity of the sound field produced by the line source can be evaluated by calculating the spatial correlation between the sound pressures at two different points. To estimate the spatial correlation of the sound pressure one must first calculate the cross-correlation function defined by

$$\mathrm{R}(k,\mathbf{x},\mathbf{y})=\mathrm{E}(p(\mathbf{x})p^*(\mathbf{y})). \tag{4}$$

This is a function of the frequency and of the two points and can be expressed as

$$\mathrm{R}(k,\mathbf{x},\mathbf{y})=\mathrm{E}\left(\int_{l_a}^{l_b}\int_{l_a}^{l_b}\frac{\mathrm{e}^{\mathrm{i}kr_x(l)}}{4\pi r_x(l)}\frac{\mathrm{e}^{-\mathrm{i}kr_y(l')}}{4\pi r_y(l')}\mu(l)\mu(l')\,\mathrm{d}l\,\mathrm{d}l'\right)=\frac{1}{(4\pi)^2}\int_{l_a}^{l_b}\frac{\mathrm{e}^{\mathrm{i}k(r_x(l)-r_y(l))}}{r_x(l)r_y(l)}\,\mathrm{d}l. \tag{5}$$

One can make the following remarks.

1. The correlation has a constant value on a circle centred on the line source and included in a plane perpendicular to the line source, because these points have the same radial distance $d=\sqrt{x_1^2+x_2^2}$ and the same x_3. This is, in fact, a consequence of the rotational invariance of the system around the axis x_3. Therefore, these points are perfectly correlated.
2. If $\mathbf{x}$ and $\mathbf{y}$ are on a straight line parallel to the line source and if this one is infinite in length ($l_a=-\infty$ and $l_b=+\infty$) the function $\mathrm{R}(k,\mathbf{x},\mathbf{y})$ is real because $d_1=d_2$ and the change $l\to -l$ transforms the integral into its conjugate.

Then the spatial correlation between the sound pressures at the two points is defined by

$$\rho(k,\mathbf{x},\mathbf{y})=|\mathrm{R}(k,\mathbf{x},\mathbf{y})|/[\mathrm{R}(k,\mathbf{x},\mathbf{x})\mathrm{R}(k,\mathbf{y},\mathbf{y})]^{1/2}. \tag{6}$$

One can see that $0\leqslant\rho(k,\mathbf{x},\mathbf{y})\leqslant 1$ and $\rho(k,\mathbf{x},\mathbf{x})=1$. What is interesting is to estimate the correlation zone around a point $\mathbf{x}$; that is, the function $\mathbf{y}\to\rho(k,\mathbf{x},\mathbf{y})$ as a function of the distance $\mathbf{x}$ to the line source and of the frequency.

2.3. BEHAVIOUR IN THE TIME DOMAIN

The results presented above were calculated in the frequency domain. However, the real control should be done in the time domain, so information on the behaviour of the system in the time domain is important. If each source emits a signal $s(l, t)$ at the abscissa l and the time t, it is possible to calculate the time signal at a point in space as

$$p(\mathbf{x}, t) = \int_{l_a}^{l_b} \frac{s(l, t - r(l)/c)}{4\pi r(l)}\,\mathrm{d}l \tag{7}$$

The intercorrelation of the signals taken at two different points is

$$\begin{aligned} \mathrm{E}(p(\mathbf{x}, t)p(\mathbf{y}, t+\tau)) &= \int_{l_a}^{l_b}\int_{l_a}^{l_b} \frac{\mathrm{E}(s(l, t - r_x(l)/c)s(l', t+\tau - r_y(l')/\mathrm{c}))}{16\pi^2 r_x(l) r_y(l')}\,\mathrm{d}l\,\mathrm{d}l' \\ &= \int_{l_a}^{l_b} \frac{\mathrm{E}(s(l, t - r_x(l)/c)s(l, t+\tau - r_y(l)/c))}{16\pi^2 r_x(l) r_y(l)}\,\mathrm{d}l \\ &= \int_{l_a}^{l_b} \frac{\mathrm{R}(l, \tau + r_x(l)/c - r_y(l)/c)}{16\pi^2 r_x(l) r_y(l)}\,\mathrm{d}l, \end{aligned} \tag{8}$$

since two sources at different positions emit independent signals. $\mathrm{R}(l, \tau)$ is the time correlation function of the source at the abscissa 1. If all the sources have the same power spectral density $S(\omega)$, the interspectrum is

$$S_{xy}(\omega) = S(\omega)\int_{l_a}^{l_b} \frac{\mathrm{e}^{-\mathrm{i}k(r_x(l) - r_y(l))}}{16\pi^2 r_x(l) r_y(l)}\,\mathrm{d}l = S(\omega)\mathrm{R}^*(k, \mathbf{x}, \mathbf{y}). \tag{9}$$

Therefore, the interspectrum between two points is equal to the spectral density of the signal emitted by the sources multiplied by the spatial correlation function. The spectral density for road traffic noise is usually a smooth function and the spectrum is large ranging from very low frequencies up to about 5000 Hz. Therefore, the spatial correlation function gives the most interesting information and will be studied in the following.

2.4. SPATIAL CORRELATION ESTIMATES

We suppose first that the source is infinite in length and try to obtain simple formulas for the spatial correlation. To estimate the domain of correlation around a point $\mathbf{x}$, one first notices, according to remark 2 in section 2.2, that in the direction x_3 the function R is real. Therefore, far from the line source, one can use the simplified expression given in Appendix A, formula (A6),

$$\mathrm{Re}\,(\mathrm{R}(k, \mathbf{x}, \mathbf{x} + r\mathbf{e}_3)) \simeq \mathrm{J}_0(kr)/16\pi d_x \tag{10}$$

and

$$\rho(k, \mathbf{x}, \mathbf{x} + r\mathbf{e}_3) \simeq \mathrm{J}_0(kr). \tag{11}$$

One has $\mathrm{J}_0(u) = 0{\cdot}5$ for $u \sim 1{\cdot}5$, so the diameter along x_3 of the zone over which the spatial correlation is greater than 0·5 is

$$2\Delta_3 \sim \lambda/2 \tag{12}$$

In the x_1 direction, one similarly has, far from the line source, the expression given in Appendix A, formula (A8),

$$\mathrm{R}(k, \mathbf{x}, \mathbf{x} + \mathrm{r}\mathbf{e}_1) \simeq \frac{1}{16\pi d_x}[\mathrm{J}_0(kr) - \mathrm{i}\mathbf{H}_0(kr)], \tag{13}$$

and

$$\rho(k, \mathbf{x}, \mathbf{x} + r\mathbf{e}_1) \simeq |\mathrm{J}_0(kr) - \mathrm{i}\mathbf{H}_0(kr)|. \tag{14}$$

$\mathbf{H}_0$ is the Struve function of order 0. One can estimate numerically the diameter along x_1 of the zone over which the spatial correlation is greater than 0·5 by

$$2\Delta_1 \sim 1{\cdot}1\lambda. \tag{15}$$

Finally, if $\mathbf{x}$ is in the x_1–x_3 plane, in the x_2 direction one uses remark 1 that the function R is constant on a circle centred on the line source and included in a perpendicular plane to show that, far from the line source, the spatial correlation is approximately constant in the x_2 direction. This fact is important because, at least in one direction, the spatial correlation remains at a value near unity. One also sees that the extent of the spatial correlation zone seems almost insensitive to the distance of the point $\mathbf{x}$ to the line source. Therefore, to be near or far from the line source does not change the extent of the spatial correlation zone, which is a function of the frequency only.

For a finite line source, in the far field, one can follow the analysis presented in Appendix A, equation (A4), to obtain

$$\mathrm{R}(k, \mathbf{x}, \mathbf{y}) \simeq \frac{1}{(4\pi)^2}\int_{l_a}^{l_b} \frac{\mathrm{e}^{-\mathrm{i}k((\varepsilon d + \eta l)/\sqrt{d^2 + l^2})}}{d^2 + l^2}\,\mathrm{d}l \simeq \frac{1}{(4\pi)^2 d}\int_{l_a/d}^{l_b/d} \frac{\mathrm{e}^{-\mathrm{i}k((\varepsilon + \eta u)/\sqrt{1 + u^2})}}{1 + u^2}\,\mathrm{d}u. \tag{16}$$

When $L = (l_b - l_a) \ll d$ one finds

$$\mathrm{R}(k, \mathbf{x}, \mathbf{y}) \simeq \frac{l_b - l_a}{(4\pi d)^2}\,\frac{\mathrm{e}^{-\mathrm{i}k((\varepsilon + \eta l_a/d)/\sqrt{1 + l_a^2/d^2})}}{1 + l_a^2/d^2}. \tag{17}$$

For these points, the spatial correlation is near unity. Therefore, when one is at a distance of the source large compared to its length the spatial correlation is restored and the system behaves like a point source. In the transition between an infinitely long source and a finite length source, one can expect that the spatial correlation increases.

2.5. DISCRETE LINE SOURCE

Instead of a continuous line source, one may be interested in the behavior of a set of discrete sources separated by a distance D and located along a straight line. This is the discrete version of the line source. In this case, the correlation function between two points is

$$\mathrm{R}_d(k, \mathbf{x}, \mathbf{y}) = \frac{D}{(4\pi)^2}\sum_{-\infty}^{+\infty} \frac{\mathrm{e}^{\mathrm{i}k(r_x(nD) - r_y(nD))}}{r_x(nD) r_y(nD)}, \tag{18}$$

with $r_x(nD) = \sqrt{d_x^2 + (x_3 - nD)^2}$ and $r_y(nD) = \sqrt{d_y^2 + (y_3 - nD)^2}$. Comparing the correlations for the continuous and discrete line sources, one has

$$\mathrm{R}(k, \mathbf{x}, \mathbf{y}) - \mathrm{R}_d(k, \mathbf{x}, \mathbf{y}) = \frac{1}{(4\pi)^2}\left[\int_{-\infty}^{+\infty} \frac{\mathrm{e}^{\mathrm{i}k(r_x(l) - r_y(l))}}{r_x(l) r_y(l)}\,\mathrm{d}l - D\sum_{-\infty}^{+\infty} \frac{\mathrm{e}^{\mathrm{i}k(r_x(nD) - r_y(nD))}}{r_x(nD) r_y(nD)}\right]$$

$$= \frac{1}{(4\pi)^2}\sum_{-\infty}^{+\infty}\int_{nD}^{(n+1)D}\left[\frac{\mathrm{e}^{\mathrm{i}k(r_x(l) - r_y(l))}}{r_x(l) r_y(l)} - \frac{\mathrm{e}^{\mathrm{i}k(r_x(nD) - r_y(nD))}}{r_x(nD) r_y(nD)}\right]\mathrm{d}l. \tag{19}$$

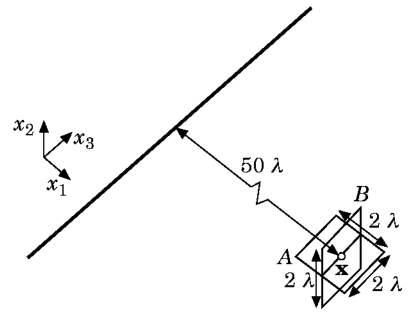

Figure 2. Cases A and B for calculation of the coherence.

In Appendix B, relation (B 10), it is shown that

$$|\mathrm{R}(k, \mathbf{x}, \mathbf{y}) - \mathrm{R}_d(k, \mathbf{x}, \mathbf{y})| \leqslant \frac{2D}{(4\pi d)^2}(k|y_3 - x_3| + 1). \tag{20}$$

Therefore, the difference is of order D/d^2, while $\mathrm{R}(k, \mathbf{x}, \mathbf{y})$ is of order $1/d$. Far from the line source $D \ll d$ and the correlation of the discrete line is identical to that of the continuous line. This means that if one is placed at a distance from the line equal to several times the distance between the point sources, the line can be considered as continuous. In the following, we will study only continuous line sources.

2.6. NUMERICAL RESULTS

To illustrate the above discussion more precisely, we have calculated the spatial correlation by a numerical integration of the function in formula (5) for an infinite line source. All distances are given in units of wavelengths. The point $\mathbf{x} = (50\lambda, 0, 0)$ is taken at 50λ from the line source. The spatial correlation is then calculated on a square of 2λ edge centred on the point $\mathbf{x}$. Two cases are studied, corresponding to Figure 2. In the first case (A) the square is included in the x_1–x_3 plane, while in the other case (B) the orientation is parallel to the x_2–x_3 plane. The results are presented in Figures 3 and 4. In the x_1–x_3 plane the domain of spatial correlation tends to concentrate around the point $\mathbf{x}$, while it is almost invariant in the x_2 direction. This supports the simplified analysis presented before and resumed by formulas (12) and (15) which estimate the spatial domain over which the correlation is greater than 0·5. This domain depends on the wavelength and looks like a cylinder in the three-dimensional space. The sound pressure is thus coherent

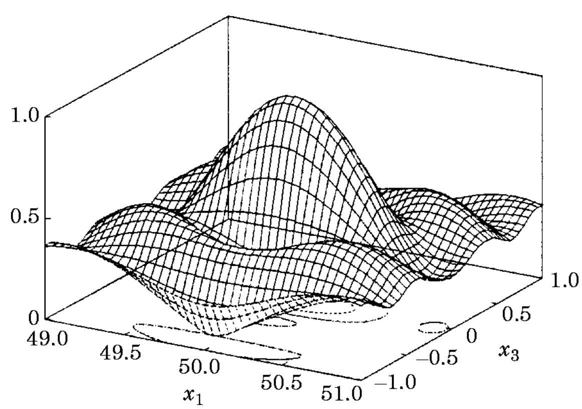

Figure 3. Case A: spatial correlation in the x_1–x_3 plane. . . . , 0·75; - - - , 0·5; – – –, 0·25.

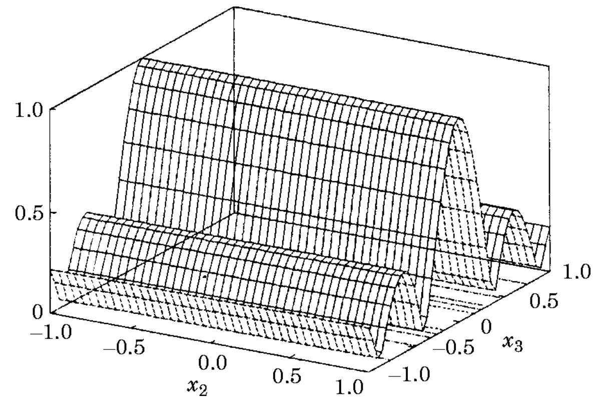

Figure 4. Case B: spatial correlation in the x_2–x_3 plane. Key as Figure 3.

over distances ranging from 17 cm (at 1000 Hz along x_3) to 3·8 m (at 100 Hz along x_1) and of course over large distances in the x_2 direction.

In the case of a finite length source, one has calculated the spatial correlation for a source of length 50λ located in the interval $[l_a = -25\lambda, l_b = 25\lambda]$. Figures 5 and 6 present the spatial correlation on the squares A and B. One can see an important improvement of the spatial correlation of the sound field when one compares them to Figures 3 and 4.

3. ACTIVE CONTROL IN FREE FIELD

The previous analysis yields large insights into the possibility of an active control in free field. If the control is realized with one error microphone and one secondary source and designed to cancel the total sound pressure at the error microphone position, one knows that the secondary sound pressure is perfectly correlated with the primary sound pressure at the error microphone position. Therefore, the domain of efficiency of the active control could not be larger than the domain of spatial correlation of the sound pressure at the cancellation point. To obtain more precise results, however, we must analyze the active control in free field and calculates its domain of efficiency.

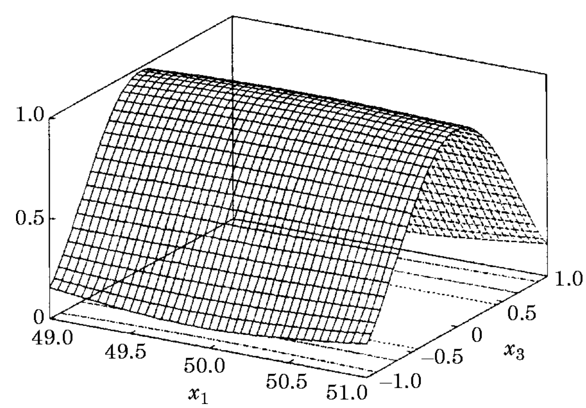

Figure 5. Spatial correlation in the x_1–x_3 plane for $L = 50\lambda$. Key as Figure 3.

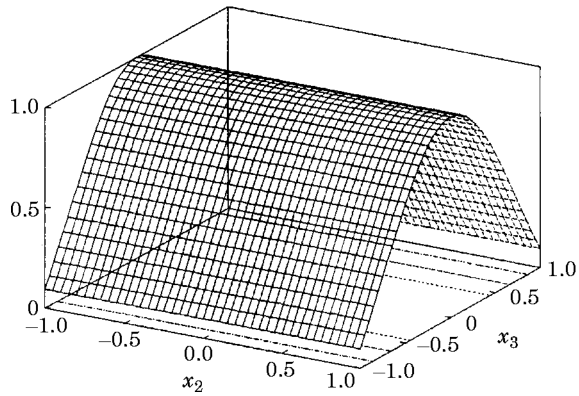

Figure 6. Spatial correlation in the x_2–x_3 plane for $L = 50\lambda$. Key as Figure 3.

3.1. CONTROL IN THE TIME DOMAIN

We have seen before, by relation (9), that the interspectrum between two points is equal to the spectral density of the signal emitted by the sources multiplied by the spatial correlation function. One knows that one channel active control with a sensor at point **x** and an error microphone at point **y** has maximal efficiency given by, if one allows non-causal controllers,

$$\gamma(\omega) = 1 - \frac{|S_{xy}(\omega)|^2}{S_{xx}(\omega) S_{yy}(\omega)} = 1 - \rho^2(k, \mathbf{x}, \mathbf{y}). \tag{21}$$

Therefore the frequency domain analysis gives the maximum efficiency of the system when using non-causal controllers and this efficiency is given by the spatial correlation function ρ. The total power before and after control at point **y** are then

$$P_{without\ control} = \int_0^\infty S(\omega)\,\mathrm{d}\omega \int_{l_a}^{l_b} \frac{1}{16\pi^2 r_y^2(l)}\,\mathrm{d}l,$$

$$P_{with\ control} = \int_0^\infty S(\omega)\,(1 - \rho^2(\omega))\,\mathrm{d}\omega \int_{l_a}^{l_b} \frac{1}{16\pi^2 r_y^2(l)}\,\mathrm{d}l \tag{22}$$

and the efficiency of the control with a non-causal controller is

$$\gamma = \int_0^\infty S(\omega)\,(1 - \rho^2(\omega))\,\mathrm{d}\omega \bigg/ \int_0^\infty S(\omega)\,\mathrm{d}\omega. \tag{23}$$

One can ask if the results are very different when using causal controllers. To give a partial answer to this question, one can calculate the optimal controller for a sensor at point **x** and an error microphone further from the line source at point $\mathbf{y} = \mathbf{x} + \varepsilon\mathbf{e}_1$, with $\varepsilon > 0$. The controller is such that

$$\mathrm{E}([\,p(\mathbf{y}, t) + h * p(\mathbf{x}, t)]^2) \tag{24}$$

is minimized and, in the frequency domain, the non-causal controller is given by

$$h(\omega) = -\frac{S_{xy}(\omega)}{S_{xx}(\omega)} = -\frac{\mathrm{R}^*(k, \mathbf{x}, \mathbf{y})}{\mathrm{R}(k, \mathbf{x}, \mathbf{x})}. \tag{25}$$

To find h in the time domain, one has to estimate the Fourier transform of R. Let us start from formula (68),

$$\mathrm{R}(k, \mathbf{x}, \mathbf{y}) \simeq \frac{1}{(4\pi)^2 d} \int_{-\infty}^{+\infty} \frac{\mathrm{e}^{-\mathrm{i}k(\varepsilon/\sqrt{1+l^2})}}{1+l^2}\,\mathrm{d}l. \tag{26}$$

With the change of variable $u = 1/\sqrt{1+l^2}$, one has

$$\mathrm{R}(k, \mathbf{x}, \mathbf{y}) \simeq \frac{2}{(4\pi)^2 d} \int_0^1 \frac{\mathrm{e}^{-\mathrm{i}k\varepsilon u}}{\sqrt{1-u^2}}\,\mathrm{d}u \tag{27}$$

and

$$h(\omega) \simeq \frac{2}{\pi} \int_0^1 \frac{\mathrm{e}^{\mathrm{i}\omega\varepsilon u/c}}{\sqrt{1-u^2}}\,\mathrm{d}u. \tag{28}$$

Therefore, finally, in the time domain, the controller is approximated by

$$h(t) \simeq \left\{\begin{matrix} \dfrac{2}{\pi}\dfrac{1}{\sqrt{(\varepsilon/c)^2 - t^2}}, & \text{if } 0 < t < \varepsilon/c \\ 0 & \text{otherwise} \end{matrix}\right\}, \tag{29}$$

and the optimal control is in fact causal in this case. For a correct placement of the points, the causality constraint does not seem to be very severe. If one takes into account the position of the secondary source, there is a non-causal part corresponding to the propagation time between the secondary source and the error microphone. However, this part should be small since the function $h(t)$ is mainly concentrated around $t = \varepsilon/c$. Therefore, the results in the frequency domain are close to the optimal possibility. As this analysis is much simpler than in the time domain, it will be the only one considered in the following.

3.2. FORMULATION IN THE FREQUENCY DOMAIN

We suppose that the active system consists of N secondary point sources positioned at points $\mathbf{S}_i$, having amplitudes a_i, and $M \geqslant N$ error microphones positioned at points $\mathbf{E}_j$. The secondary sources are driven to minimize the sum of the squared pressures at error microphones, that is the cost function

$$\mathrm{J} = \sum_{j=1}^{M} |p_p(\mathbf{E}_j) + p_s(\mathbf{E}_j)|^2, \tag{30}$$

where $p_p(\mathbf{E}_j)$ is the primary sound pressure coming from the line source and $p_s(\mathbf{E}_j)$ is the secondary sound pressure produced by the secondary point sources. This secondary sound pressure is given by

$$p_s(\mathbf{E}_j) = \sum_{i=1}^{N} a_i \frac{\mathrm{e}^{\mathrm{i}kr_{ji}}}{4\pi r_{ji}}, \tag{31}$$

where $r_{ji} = |\mathbf{E}_j - \mathbf{S}_i|$ is the distance between the error microphone j and the secondary source i. Upon denoting

$$T_{ji} = \frac{\mathrm{e}^{\mathrm{i}kr_{ji}}}{4\pi r_{ji}} \tag{32}$$

the matrix of transfer functions and

$$P_j = p_p(\mathbf{E}_j), \tag{33}$$

the vector of primary sound pressures at error microphones, the cost function can be written as

$$J = \mathbf{P}^{\mathrm{H}}\mathbf{P} + \mathbf{P}^{\mathrm{H}}\mathbf{T}\mathbf{A} + \mathbf{A}^{\mathrm{H}}\mathbf{T}^{\mathrm{H}}\mathbf{P} + \mathbf{A}^{\mathrm{H}}\mathbf{T}^{\mathrm{H}}\mathbf{T}\mathbf{A}. \tag{34}$$

This quadratic form is minimum for the vector of secondary source amplitudes $\mathbf{A}$ given by

$$\mathbf{A} = -[\mathbf{T}^{\mathrm{H}}\mathbf{T}]^{-1}\mathbf{T}^{\mathrm{H}}\mathbf{P} = -\mathbf{G}\mathbf{P}, \tag{35}$$

where $\mathbf{G} = [\mathbf{T}^{\mathrm{H}}\mathbf{T}]^{-1}\mathbf{T}^{\mathrm{H}}$. Therefore, the total sound pressure at a point $\mathbf{x}$ after control is

$$p_p(\mathbf{x}) + \sum_{i=1}^{N} a_i \frac{\mathrm{e}^{\mathrm{i}kr_i}}{4\pi r_i} = p_p(\mathbf{x}) - \sum_{i=1}^{N} \frac{\mathrm{e}^{\mathrm{i}kr_i}}{4\pi r_i} \sum_{j=1}^{M} G_{ij} P_j = p_p(\mathbf{x}) - \sum_{j=1}^{M}\left[\sum_{i=1}^{N} \frac{\mathrm{e}^{\mathrm{i}kr_i}}{4\pi r_i} G_{ij}\right] P_j$$

$$= p_p(\mathbf{x}) - \sum_{j=1}^{M} H_j(\mathbf{x}) P_j = p_p(\mathbf{x}) - \mathbf{H}^{\mathrm{T}}(\mathbf{x})\mathbf{P}, \tag{36}$$

with $r_i = |\mathbf{x} - \mathbf{S}_i|$ and

$$H_j(\mathbf{x}) = \sum_{i=1}^{N} \frac{\mathrm{e}^{\mathrm{i}kr_i}}{4\pi r_i} G_{ij}.$$

Finally, the density of acoustic potential energy at point $\mathbf{x}$ after control is

$$e_c = \mathrm{E}\left(\frac{|p_p(\mathbf{x}) + p_s(\mathbf{x})|^2}{4\rho c^2}\right) = \frac{1}{4\rho c^2}\left[R(k, \mathbf{x}, \mathbf{x}) - \sum_{j=1}^{M} H_j^* R(k, \mathbf{x}, \mathbf{E}_j)\right.$$

$$\left. - \sum_{j=1}^{M} H_j R(k, \mathbf{E}_j, \mathbf{x}) + \sum_{j=1}^{M}\sum_{k=1}^{M} H_j^* H_k R(k, \mathbf{E}_k, \mathbf{E}_j)\right]. \tag{37}$$

With

$$e_p = \mathrm{E}(|p_p(\mathbf{x})|^2/4\rho c^2)$$

being the energy density of the primary field, the energy reduction is

$$\frac{e_c}{e_p} = 1 - \sum_{j=1}^{M} H_j^* \frac{R(k, \mathbf{x}, \mathbf{E}_j)}{R(k, \mathbf{x}, \mathbf{x})}$$

$$- \sum_{j=1}^{M} H_j \frac{R(k, \mathbf{E}_j, \mathbf{x})}{R(k, \mathbf{x}, \mathbf{x})} + \sum_{j=1}^{M}\sum_{k=1}^{M} H_j^* H_k \frac{R(k, \mathbf{E}_k, \mathbf{E}_j)}{R(k, \mathbf{x}, \mathbf{x})}. \tag{38}$$

3.3. CONTROL LENGTH ESTIMATES

In the special case of a control with one secondary source and one error microphone, one obtains $G_{11} = 4\pi r_{11}\,\mathrm{e}^{-ikr_{11}}$ and $H_1 = (r_{11}/r)\,\mathrm{e}^{ik(r-r_{11})}$, where $r_{11} = |\mathbf{E} - \mathbf{S}|$ and $r = |\mathbf{x} - \mathbf{S}|$. Far from the line source the distances of the error microphone and of the point $\mathbf{x}$ to the line source are equal, and denoted d, up to terms or order $|\mathbf{E} - \mathbf{x}|/d$ which are neglected. This leads to

$$e_c/e_p \simeq 1 - 32\pi d\,\mathrm{Re}\,[(r_{11}/r)\,\mathrm{e}^{ik(r_{11}-r)}\mathrm{R}(k, \mathbf{x}, \mathbf{E})] + (r_{11}/r)^2. \tag{39}$$

To simplify one studies the case, where $\mathbf{E} - \mathbf{S}$ is parallel to x_1. As for the spatial correlation, one can estimate the domain of control by calculating the potential energy reduction for points on straight lines parallel to the co-ordinate axes. In the x_1 direction, noting that $\varepsilon = x_1 - x_1^e$, using a development of $\mathrm{R}(k, \mathbf{x}, \mathbf{E})$ from the formulas of Appendix A and supposing, furthermore, that the secondary source is at several wavelengths from the error microphone one finally obtains

$$\frac{e_c}{e_p} \simeq \left(\frac{3}{2} - \frac{4}{\pi}\right)(k\varepsilon)^2. \tag{40}$$

In this case, one can estimate the diameter of the zone over which the pressure is reduced by more than 10 dB as

$$2\Delta_1 \simeq \lambda/5. \tag{41}$$

In the same way, in the x_3 direction one has, upon noting $\eta = x_3 - x_3^e$,

$$e_c/e_p \simeq (k\eta)^2/2. \tag{42}$$

The diameter along x_3 of the -10 dB zone is

$$2\Delta_3 \simeq \lambda/7. \tag{43}$$

Finally, in the x_2 direction one gets, with $\mu = x_2 - x_2^e$,

$$e_c/e_p \simeq k^2\mu^4/4r_{11}^2, \tag{44}$$

and the diameter is

$$2\Delta_2 \simeq 0{\cdot}6\sqrt{\lambda r_{11}}. \tag{45}$$

3.4. NUMERICAL RESULTS

To verify these calculations the attenuation has been determined on the two squares of Figure 2 for a secondary source placed at point $(45\lambda, 0, 0)$ and an error microphone at the center of the squares at point $(50\lambda, 0, 0)$. The correlation is calculated by the formula (5) upon supposing first that the line source is infinite in length. Figures 7 and 8 present the attenuation in the x_1–x_3 and x_2–x_3 planes and confirm the previous estimations on the size of the cancellation zone. The maximum attenuation has been limited to 25 dB to improve the clarity of the figures. The cancellation zone has a small extent in the x_1 and x_3 directions but is much larger in the x_2 direction. The sound pressure can increase outside the quiet zone.

It was shown by Wright and Vuksanovic [3] that for a control of a primary point source in free field by another point source the cancellation zone looks like an angular sector of axis x_1 and with an aperture depending on the spatial arrangement of the system and on the frequency. When the error microphone is far enough from the secondary source relatively large zones of silence can be obtained with, for instance, an acoustic shadow

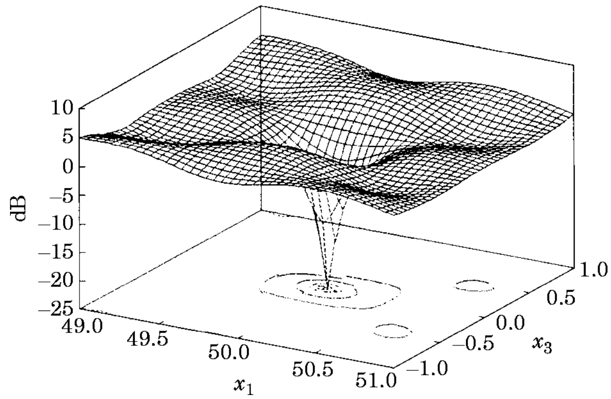

Figure 7. Attenuation in the x_1–x_3 plane with one secondary source. . . . . . , 5; —, 0; –·–· , -5; –·–·–·–, -10; ·· ·· ·· ··, -15; ·· ···, -20; ···· ····, -25.

along x_1. One finds here much smaller dimensions along x_1 and x_3 because of the poor correlation of the sound field in these directions. On the contrary, along x_2 the good correlation leads to a situation similar to the case studied by Wright *et al*. [3] and should allow similar control zones.

To try to extend the quiet zone, another calculation was made with five secondary sources placed at points $(45\lambda, 0, -5\lambda)$, $(45\lambda, 0, -2{\cdot}5\lambda)$, $(45\lambda, 0, 0)$, $(45\lambda, 0, 2{\cdot}5\lambda)$, $(45\lambda, 0, 5\lambda)$. Five error microphones are placed at points $(50\lambda, 0, -0{\cdot}4\lambda)$, $(50\lambda, 0, -0{\cdot}2\lambda)$, $(50\lambda, 0, 0)$, $(50\lambda, 0, 0{\cdot}2\lambda)$, $(50\lambda, 0, 0{\cdot}4\lambda)$. The distance between the microphones has been chosen according to formula (43) to give an overlapping of the attenuation zone of the microphones. The results are shown in Figures 9 and 10. The cancellation zone has been extended in comparison to the case with one microphone. Other simulations not given here were done with a larger distance between the microphones. It was observed that the control tends to be localized around the error microphones with an increase of the sound level elsewhere. Therefore, to really control a large zone, the distances between the microphones should be of the same order as that given by relations (41) and (43). The positions of the secondary sources seem less important.

Simulations are now presented for finite length sources with the correlation function defined by equation (5) and the source symmetrical around the origin; that is, $l_a = -l_b$. We again calculate the examples of Figures 7 and 8 with a line of length 50λ. The results

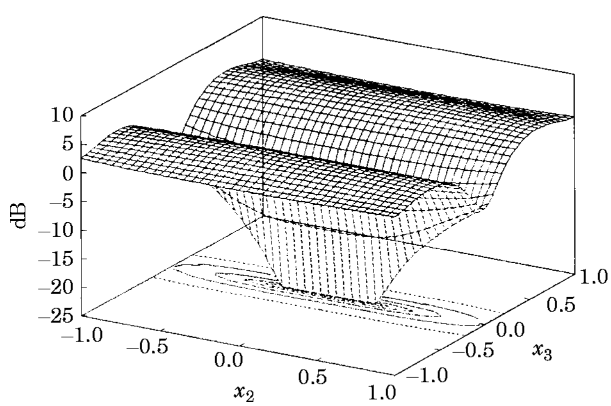

Figure 8. Attenuation in the x_2–x_3 plane with one secondary source. Key as Figure 7.

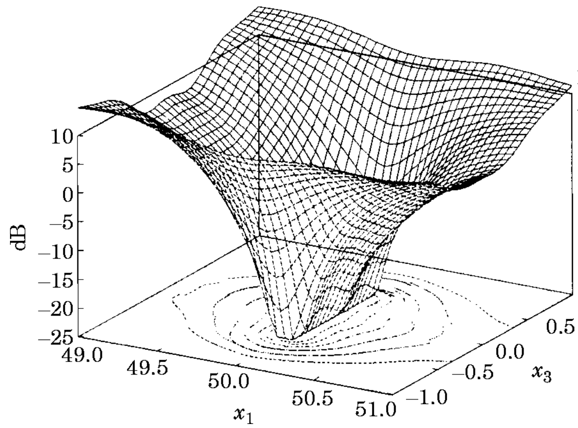

Figure 9. Attenuation in the x_1–x_3 plane with five secondary sources. Key as Figure 7.

are presented in Figures 11 and 12, and considerable improvements over the infinite line source can be seen in each case because the spatial extent of the attenuation zone is much larger.

To show the influence of the source length, the efficiency of the active control is calculated in the x_1–x_3 plane, in the x_3 direction, for different source lengths. The results are presented in Figure 13 for the lengths 2λ, 25λ, 50λ, 100λ and an infinite length. One can see the deterioration of the attenuation as the length increases and conclude from these results that a decrease in the length of the source leads to considerable improvement in the active control efficiency.

For a given source length, one can try to put the active system at a larger distance from the line source. To test this hypothesis, we carried out the same calculation but the secondary source is now at the distance 95λ from the line source while the error microphone is at 100λ. The results are presented in Figure 14. Comparison with Figure 13 shows important differences for sources of length 25λ, 50λ and 100λ, while there is little difference for the source length 2λ. In this latter case, it seems that the active system is far enough to be able to consider the source as a point source for both distances. On the contrary, for the source lengths 25λ, 50λ and 100λ, a change in the distance between the active system and the line source has an important effect on the angle at which the source

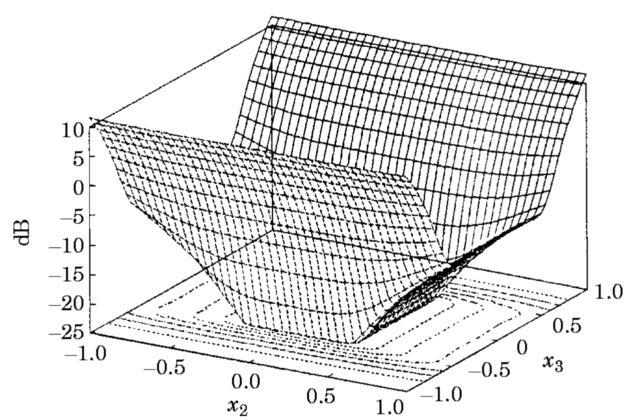

Figure 10. Attenuation in the x_2–x_3 plane with five secondary sources. Key as Figure 7.

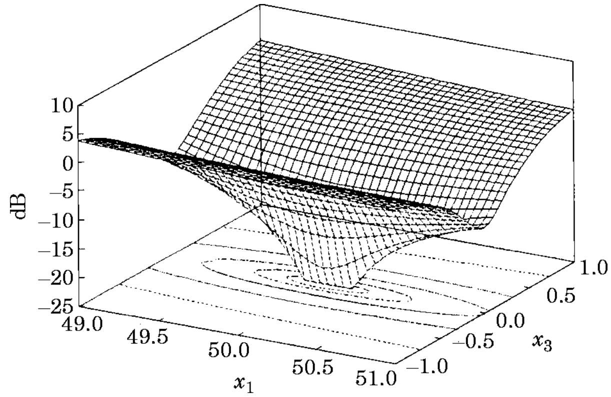

Figure 11. Attenuation in the x_1–x_3 plane for $L = 50\lambda$. Key as Figure 7

is seen from the error microphone. As one moves further from the source, the spatial correlation of the primary field is increased and the noise reduction is better. Therefore, for a given source length, one should place the active control system as far as possible from the line source.

4. DIFFRACTION BY AN APERTURE

The previous discussion on the active control in free field revealed that the cancellation zone is relatively small and has dimensions decreasing with the frequency. Therefore, it seems difficult to reduce the sound pressure over large spatial zones with a reasonable number of microphones and secondary sources. However, the active control could be efficient enough to significantly reduce the sound pressure crossing an aperture in a screen. The aperture could for instance be a model for an open window which receives the sound pressure created by a road traffic modelled by the incoherent line source. To investigate this problem in more details, one must first be able to calculate the energy transmission across the aperture, then one has to estimate the efficiency of an active control for various secondary source and microphone arrangements.

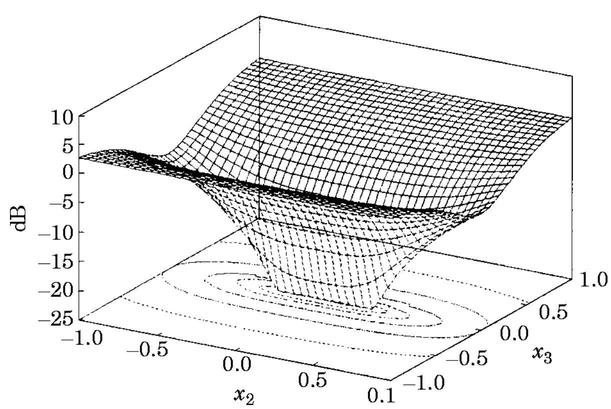

Figure 12. Attenuation in the x_2–x_3 plane for $L = 50\lambda$. Key as Figure 7

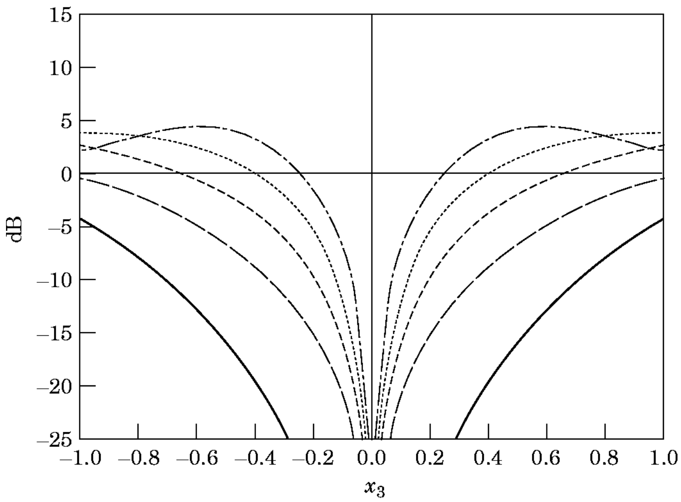

Figure 13. Attenuation with source length for $d = 50\lambda$. L values: ——, 2; — — —, 25; – – –, 50; · · · ·, 100; — · — ·, infinity.

4.1. ENERGY TRANSMISSION

We propose first to determine the energy transmission across an aperture D in a rigid screen (see Figure 15). The noise sources are located on one side of the screen and one is interested in the transmission of energy to the other side through the aperture.

The incident sound pressure is denoted by $p_{inc}(\mathbf{x})$; this is the sound pressure created by the source in free field. The total sound pressure, denoted $p(\mathbf{x})$, includes the diffraction by the rigid plane and the aperture. According to Babinet's principle (see, for instance, reference [13]), one knows that the total sound pressure on the aperture is the same as the incident pressure, that is,

$$p(\mathbf{x}) = p_{inc}(\mathbf{x}) \qquad \text{for } \mathbf{x} \in D. \tag{46}$$

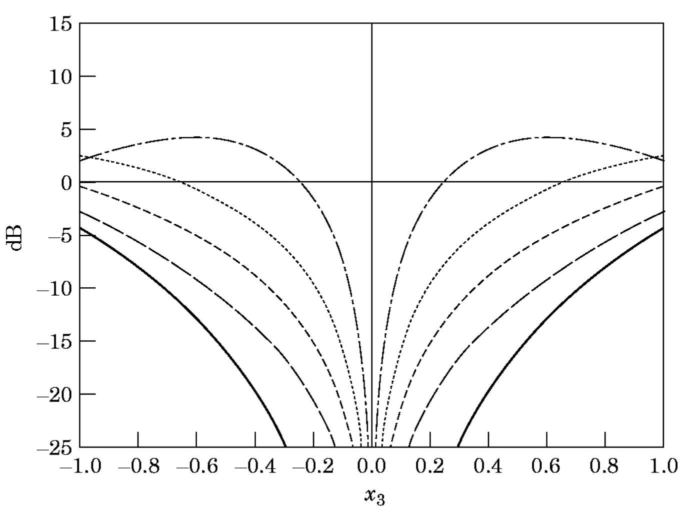

Figure 14. Attenuation with source length for $d = 100\lambda$. Key as Figure 13.

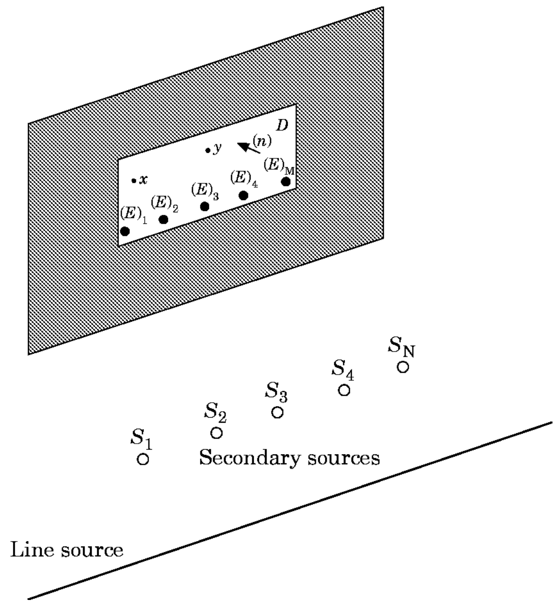

Figure 15. Aperture in a rigid plane.

Therefore, on the aperture D, the pressure is the solution of the integral equation

$$p_{inc}(\mathbf{x}) = -\int_D G(\mathbf{x}, \mathbf{y}) \frac{\partial p}{\partial n}(\mathbf{y})\, \mathrm{d}\mathbf{y} \qquad \text{for } \mathbf{x} \in D, \tag{47}$$

where $G(\mathbf{x}, \mathbf{y})$ is the Green function for a rigid boundary condition on the half-plane given by

$$G(\mathbf{x}, \mathbf{y}) = \frac{\mathrm{e}^{ik|\mathbf{x}-\mathbf{y}|}}{4\pi|\mathbf{x}-\mathbf{y}|} + \frac{\mathrm{e}^{ik|\mathbf{x}-\mathbf{y}'|}}{4\pi|\mathbf{x}-\mathbf{y}'|}, \tag{48}$$

in which $\mathbf{y}'$ is symmetric to $\mathbf{y}$ with respect to the screen. The boundary equation is solved by the boundary element method by using quadrangular four nodes elements (see Figure 16). We took about five nodes per wavelength.

Therefore, the pressure and its normal derivative are approximated by

$$p(\mathbf{x}) = \sum_{i=1}^{N} p_i N_i(\mathbf{x}), \qquad \frac{\partial p}{\partial n}(\mathbf{x}) = \sum_{i=1}^{n} q_i N_i(\mathbf{x}), \tag{49}$$

where p_i and q_i are respectively the nodal values of the pressure and the normal derivative of the pressure and N_i are the interpolation functions. The boundary integral equation was

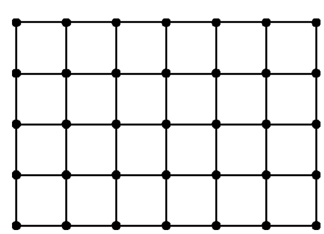
Figure 16. Mesh of the aperture

solved by the collocation method. Therefore equation (47) was used for $\mathbf{x} = \mathbf{x}_i$ and the integral over D was decomposed over the elements of the mesh:

$$p_{inc}(\mathbf{x}_i) = -\int_D G(\mathbf{x}_i, \mathbf{y}) \frac{\partial p}{\partial n}(\mathbf{y})\,\mathrm{d}\mathbf{y}, \qquad p_i = \sum_{j=1}^{n} Z_{ij}\, q_j, \tag{50, 51}$$

where

$$Z_{ij} = -\int_D G(\mathbf{x}_i, \mathbf{y}) N_j(\mathbf{y})\,\mathrm{d}\mathbf{y}. \tag{52}$$

These matrix elements were calculated by Gauss integration. Special care should be taken in the evaluation of Z_{ii} because of the singularity in the Green function. Thus one has the nodal values of the normal derivative ${}^t\mathbf{Q} = {}^t(q_1, \ldots, q_n)$ as a function of the pressure ${}^t\mathbf{P} = {}^t(p_1, \ldots, p_n)$ as

$$\mathbf{Q} = \mathbf{Z}^{-1}\mathbf{P}. \tag{53}$$

The energy radiated by the aperture can then be calculated as

$$e = \tfrac{1}{2}\int_D \mathrm{Re}\,(p^*(\mathbf{x})\mathbf{v}(\mathbf{x}) \cdot \mathbf{n}(\mathbf{x}))\,\mathrm{d}\mathbf{x} = \frac{1}{2\rho\omega}\int_D \mathrm{Im}\left(p^*(\mathbf{x})\frac{\partial p}{\partial n}(\mathbf{x})\right)\mathrm{d}\mathbf{x}. \tag{54}$$

In terms of the nodal values of the pressure the energy is

$$e = \frac{1}{2\rho\omega}\int_D \mathrm{Im}\left[\left(\sum_{i=1}^{n} p_i^* N_i(\mathbf{x})\right)\cdot\left(\sum_{j,k=1}^{n} Z_{jk}^{-1} p_k N_j(\mathbf{x})\right)\right]\mathrm{d}\mathbf{x}$$

$$= \frac{1}{2\rho\omega}\sum_{i,k=1}^{n} \mathrm{Im}\,[(MZ^{-1})_{ik}\, p_i^*\, p_k], \tag{55}$$

where the matrix $\mathbf{M}$ is defined by $M_{ij} = \int_D N_i(\mathbf{x}) N_j(\mathbf{x})\,\mathrm{d}\mathbf{x}$. Upon supposing now that the incident sound pressure comes from an incoherent line source, the nodal values of the incident pressure are random variables and one must calculate the expectation of the energy radiated. One has, for the average energy,

$$\bar{e} = \frac{1}{2\rho\omega}\,\mathrm{E}\left(\sum_{i,k=1}^{n} \mathrm{Im}\,[(MZ^{-1})_{ik}\, p_i^*\, p_k]\right) = \frac{1}{2\rho\omega}\sum_{i,k=1}^{n} \mathrm{Im}\,[(MZ^{-1})_{ik}\,\mathrm{E}(p_i^*\, p_k)]$$

$$= \frac{1}{2\rho\omega}\sum_{i,k=1}^{n} \mathrm{Im}\,[(MZ^{-1})_{ik}\,\mathrm{R}(k, \mathbf{x}_k, \mathbf{x}_i)], \tag{56}$$

where we have introduced the correlation function R previously calculated.

4.2. ACTIVE CONTROL OF THE SOUND TRANSMISSION

We now want to reduce the energy transmission across the aperture with an active control system. It consists of secondary sources and error microphones. We suppose that the error microphones are positioned on the aperture D where they will create zones of minimum sound pressure (see Figure 15). The secondary sources are positioned between the line source and the screen. We will calculate the maximum efficiency of the system:

that is, the optimal secondary source amplitudes which minimize the sound pressure at the error microphones, and then the energy transmission with control.

We suppose, as in the free field case, that the secondary sources are point sources. Therefore, they produce the incident secondary field

$$p_s(\mathbf{r}) = \sum_{i=1}^{N} a_i \frac{\mathrm{e}^{\mathrm{i}kr_i}}{4\pi r_i}, \tag{57}$$

where $r_i = |\mathbf{r} - \mathbf{S}_i|$ is the distance between the point $\mathbf{r}$ and the secondary source $\mathbf{S}_i$. N is the number of secondary sources. M denotes the number of error microphones and we suppose that $M \geqslant N$. The error microphones are placed on the aperture D so that, according to Babinet's principle, the total and incident pressures at the error microphones are the same. The vector of primary pressures at the error microphones is called $\mathbf{P}_e^{\mathrm{T}} = (p_p(\mathbf{E}_1), \ldots, p_p(\mathbf{E}_M))^{\mathrm{T}}$, where $p_p(\mathbf{E}_j)$ is the primary pressure at the error microphone position $\mathbf{E}_j$. The secondary source amplitudes that minimize the sound pressure at the error microphones minimize the quadratic form

$$J = (\mathbf{P}_e + \mathbf{TA})^{\mathrm{H}}(\mathbf{P}_e + \mathbf{TA}), \tag{58}$$

where $\mathbf{A}^{\mathrm{T}} = (a_1, \ldots, a_N)^{\mathrm{T}}$ are the amplitudes of the secondary sources and

$$T_{ji} = \mathrm{e}^{\mathrm{i}kr_{ji}/4\pi r_{ji}} \qquad \text{with} \;\; r_{ji} = |\mathbf{E}_j - \mathbf{S}_i|. \tag{59}$$

Therefore, one has

$$\mathbf{A} = -[\mathbf{T}^{\mathrm{H}}\mathbf{T}]^{-1}\mathbf{T}^{\mathrm{H}}\mathbf{P}_e. \tag{60}$$

With this result, one can now calculate the incident pressure at the mesh nodes which is the sum of the contributions of the primary and secondary sources. At the node position $\mathbf{x}_k$ the incident pressure is

$$p_{inc}(\mathbf{x}_k) = p_p(\mathbf{x}_k) + \sum_{i=1}^{N} a_i \frac{\mathrm{e}^{\mathrm{i}kr_{ki}}}{4\pi r_{ki}}, \tag{61}$$

with $r_{ki} = |\mathbf{x}_k - \mathbf{S}_i|$. Therefore, the nodal values of the incident pressure are given by the vector

$$\mathbf{P} - \tilde{\mathbf{T}}[\mathbf{T}^{\mathrm{H}}\mathbf{T}]^{-1}\mathbf{T}^{\mathrm{H}}\mathbf{DP} = \mathbf{KP}, \tag{62}$$

with $\tilde{T}_{ki} = \mathrm{e}^{\mathrm{i}kr_{ki}}/4\pi r_{ki}$, $P_k = p(\mathbf{x}_k)$ and $\mathbf{D}$ is a matrix doing the link between the microphone and the node numbers. $D_{jk} = 1$ if the microphone number j is at node number k and 0 elsewhere, so that $\mathbf{P}_e = \mathbf{DP}$. The definition of the matrix $\mathbf{K}$ follows from formula (62). Therefore, one sees that the action of the active control consists in changing the vector of the incident pressure from $\mathbf{P}$ to $\mathbf{KP}$. Application of formula (56) gives the energy radiated with control as

$$\bar{e}_c = \frac{1}{2\rho\omega} \sum_{i,k=1}^{n} \mathrm{Im}\,[(MZ^{-1})_{ik}\,(KRK^{\mathrm{H}})_{ki}]. \tag{63}$$

The attenuation provided by the active control is finally given by

$$At = 10 \log_{10}(\bar{e}_c/\bar{e}), \tag{64}$$

where the energy radiated without control $\bar{e}$ is calculated by formula (56).

4.3. NUMERICAL RESULTS

We now present calculation of the attenuation of the energy transmission for some examples of aperture and active systems arrangements. The aperture is located in the x_2–x_3 plane with corners at points (50, $-0{\cdot}5$, $-0{\cdot}5$), (50, $0{\cdot}5$, $-0{\cdot}5$), (50, $0{\cdot}5$, $0{\cdot}5$), (50, $-0{\cdot}5$, $0{\cdot}5$). The distances are given here in meters, so the aperture is a square of side 1 m. We calculate the efficiency of the active control for systems with one to four secondary sources using the same number of error microphones as secondary sources. The microphones are positioned at point (50, 0, 0) for a unique microphone, at points (50, 0, $-0{\cdot}25$) and (50, 0, $0{\cdot}25$) for two microphones, at points (50, 0, $-1/3$), (50, 0, 0) and (50, 0, 1/3) for a system with three microphones and at points (50, 0, $-0{\cdot}375$), (50, 0, $-0{\cdot}125$), (50, 0, $0{\cdot}125$) and (50, 0, $0{\cdot}375$) for a system with four microphones. The secondary sources are placed at the abscissa $x_1 = 45$ m with the same x_3 co-ordinate as the error microphones. The results are presented in Figure 17, it being first supposed that the line source is infinite. The attenuation is presented as a function of a/λ, where λ is the wavelength and $a = 1$ m is the dimension of the aperture. The frequency range is between 20 Hz and 1000 Hz. As expected, the attenuation is a decreasing function of the frequency. The control is efficient (-10 dB of attenuation at least) approximately until $a/\lambda \simeq n/3$. In other words, each microphone contributes to the control over a distance of $\lambda/3$ and one obtains a good control when there are enough microphones to fill the aperture. One must have as many secondary sources as microphones.

For the case of a finite source of length 50 m, the results are presented in Figure 18. The active systems are the same as before. Now each source contributes to the control over a distance approximately equal to $0{\cdot}7\lambda$. Because of the spatial correlation properties of the sound field a line of secondary sources is thus able to control the energy transmission across a whole surface, thus avoiding the covering of a complete surface with control sources. The difference between the finite and infinite line source shows that the spatial correlation of the primary pressure field has important effects on the efficiency of the system.

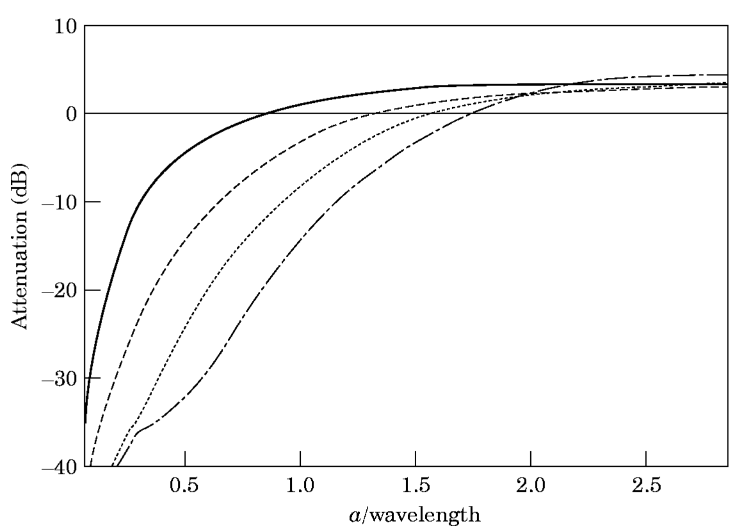

Figure 17. Attenuation for an infinite line source. ——, 1 source; - - -, 2 sources; · · · ·, 3 sources; — - —, 4 sources.

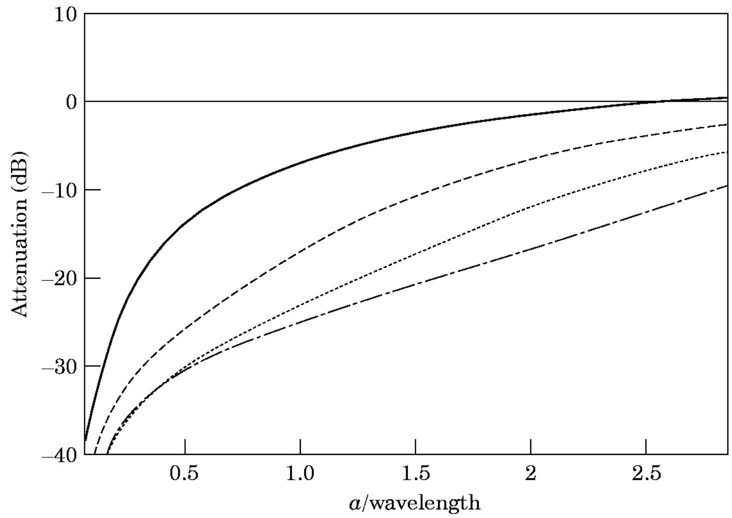

Figure 18. Attenuation for a finite line source with $L = 50$ m. Key as Figure 17.

4.4. CONTROL SYSTEM

The results presented here were mainly obtained in the frequency domain by supposing that the primary source was harmonic. They give the maximum attenuation that can be obtained at a specified frequency component of the pressure field for a geometrical arrangement of the system. In one example, it was seen that with a proper arrangement of the system the causality constraint does not seem to be very severe and should not change drastically the obtained results. For the control of moving sources, the Doppler effect can change some properties of the signals. However, the movement of the source is perpendicular to the observer and in this case the Doppler effect is mimimized.

For real-time control, it is necessary to implement a control algorithm. Because of the poor correlation of the primary field it seems that simple systems made of a small number of sensor microphones should rather be built with feedback algorithms. To build a feedforward controller one would need many sensors to obtain a primary reference signal well correlated with the error microphone signals. The detailed analysis of these questions is left for future works. Anyway, no matter how the active control is obtained, the analysis presented gives an answer to the question: ‘‘What maximum control can be obtained with a specified arrangement of error sensors and secondary sources?’’

5. CONCLUSION

The previous study has shown that the active control of the noise created by transport systems could be possible at least in a limited space domain. The extent of the quiet zone depends both on the frequency and on the length of the source. Therefore, for an infinite source length the quiet zone has dimensions of a fraction of a wavelength. But for limited source lengths considerable improvement on the efficiency of the control could be obtained. Similar conclusions are driven for the energy transmission into an aperture. It could be substantially reduced for low frequencies with a few secondary sources and error microphones.

ACKNOWLEDGMENTS

The authors gratefully acknowledge the financial support of this research from the ASFA (Association des Sociétés Françaises d'Autoroutes). They also thank the anonymous referees for their suggestions to improve this paper.

REFERENCES

1. P. A. NELSON, A. R. D. CURTIS, S. J. ELLIOTT and A. J. BULLMORE 1987 *Journal of Sound and Vibration* **116**, 397–414. The minimum power output of free field point sources and the active control of sound.
2. M. O. TOKHI 1995 *International Journal of Active Control* **1**, 109–144. Analysis and robust design of active noise control systems incorporating compact sources.
3. S. E. WRIGHT and B. VUKSANOVIC 1996 *Journal of Sound and Vibration* **190**, 565–585. Active control of environmental noise.
4. S. ISE, H. YANO and H. TACHIBANA 1991 *Journal of the Acoustical Society of Japan* **12**, 299–306. Basic study on active noise barrier.
5. A. OMOTO and K. FUJIWARA 1993 *Journal of the Acoustical Society of America* **94**, 2173–2180. A study of an actively controlled noise barrier.
6. A. OMOTO, K. TAKASHIMA, K. FUJIWARA, M. AOKI and Y. SHIMIZU 1994 in *Inter-noise* 94, *Yokohama*, 29–31 *August*, 1357–1360. Active suppression of sound diffracted by barrier: experiment in the outdoors.
7. D. DUHAMEL 1995 *Acta Acustica* **3**, 25–35. Improvement of noise barrier efficiency by active control.
8. P. JOSEPH, S. J. ELLIOTT and P. A. NELSON 1994 *Journal of Sound and Vibration* **172**, 605–627. Near field zones of quiet.
9. P. JOSEPH, S. J. ELLIOTT and P. A. NELSON 1994 *Journal of Sound and Vibration* **172**, 629–655. Statistical aspects of active control in harmonic enclosed sound fields.
10. S. J. ELLIOTT, P. JOSEPH, A. J. BULLMORE and P. A. NELSON 1988 *Journal of Sound and Vibration* **120**, 183–189. Active cancellation at a point in a pure tone diffuse sound field.
11. J. GARCIA-BONITO and S. J. ELLIOTT 1995 *Journal of the Acoustical Society of America* **98**, 1017–1024. Local active control of diffracted diffuse sound field.
12. A. DAVID and S. J. ELLIOTT 1994 *Applied Acoustics* **41**, 63–79. Numerical studies of actively generated quiet zones.
13. E. SKUDRZYK 1971 *The Foundations of Acoustics*. Berlin: Springer-Verlag.
14. M. ABRAMOWITZ and I. A. STEGUN 1972 *Handbook of Mathematical Functions*. New York: Dover.

APPENDIX A: ASYMPTOTIC FORMULA FOR THE CORRELATION

The correlation function for an infinite source is given by

$$\mathrm{R}(k, \mathbf{x}, \mathbf{y}) = \frac{1}{(4\pi)^2} \int_{-\infty}^{+\infty} \frac{\mathrm{e}^{\mathrm{i}k(r_x(l) - r_y(l))}}{r_x(l) r_y(l)} \, \mathrm{d}l. \tag{A1}$$

One looks for an asymptotic formula far from the line source. Calling $d = \sqrt{x_1^2 + x_2^2}$ the radial distance of point x to the line source and supposing that

$$d_y = d + \varepsilon, \quad y_3 = x_3 - \eta, \tag{A2}$$

with $|\varepsilon| \ll d$ and $|\eta| \ll d$, one has the developments (with the origin in 1 at $(x_3 + y_3/2)$),

$$r_x(l) = \sqrt{d^2 + \left(l - \frac{\eta}{2}\right)^2} = \sqrt{d^2 + l^2}\left(1 - \frac{\eta l}{2(d^2 + l^2)} + O\left(\frac{\eta^2}{d^2}\right)\right),$$

$$r_y(l) = \sqrt{(d + \varepsilon)^2 + \left(l + \frac{\eta}{2}\right)^2} = \sqrt{d^2 + l^2}\left(1 + \frac{\varepsilon d}{d^2 + l^2} + \frac{\eta l}{2(d^2 + l^2)} + O\left(\frac{\varepsilon^2 + \eta^2}{d^2}\right)\right). \quad \text{(A3)}$$

Therefore, one finds that

$$\mathrm{R}(k, \mathbf{x}, \mathbf{y}) \simeq \frac{1}{(4\pi)^2}\int_{-\infty}^{+\infty} \frac{\mathrm{e}^{-\mathrm{i}k((\varepsilon d + \eta l)/\sqrt{l^2 + d^2})}}{d^2 + l^2}\left(1 - \frac{\varepsilon d}{d^2 + l^2}\right)\mathrm{d}l, \quad \text{(A4)}$$

and with the change of variable $l = d\tan\theta$, one has

$$\mathrm{R}(k, \mathbf{x}, \mathbf{y}) \simeq \frac{1}{(4\pi)^2 d}\int_{-\pi/2}^{\pi/2} \mathrm{e}^{-\mathrm{i}k(\varepsilon\cos\theta + \eta\sin\theta)}\left(1 - \frac{\varepsilon}{d}\cos^2\theta\right)\mathrm{d}\theta. \quad \text{(A5)}$$

One can calculate the real part of this expression to order 0 in ε/d by

$$\mathrm{Re}\,(\mathrm{R}(k, \mathbf{x}, \mathbf{y})) \simeq \frac{1}{(4\pi)^2 d}\int_{-\pi/2}^{\pi/2} \cos(k(\varepsilon\cos\theta + \eta\sin\theta))\,\mathrm{d}\theta$$

$$\simeq \frac{1}{(4\pi)^2 2d}\int_{-\pi}^{\pi} \cos(k(\varepsilon\cos\theta + \eta\sin\theta))\,\mathrm{d}\theta \simeq \frac{1}{(4\pi)^2 2d}$$

$$\times \int_0^{2\pi} \cos(kr\cos\theta)\,\mathrm{d}\theta \simeq \frac{1}{(4\pi)^2 d}\int_0^{\pi} \cos(kr\cos\theta)\,\mathrm{d}\theta \simeq \frac{\mathrm{J}_0(kr)}{16\pi d}, \quad \text{(A6)}$$

where $r = \sqrt{\varepsilon^2 + \eta^2}$ and J_0 is the Bessel function of order 0.

One can also calculate the imaginary part for points such as $\eta = 0$. In this case, to order 0 in ε/d,

$$\mathrm{Im}\,(\mathrm{R}(k, \mathbf{x}, \mathbf{y})) \simeq \frac{1}{(4\pi)^2 d}\int_{-\pi/2}^{\pi/2} -\sin(k\varepsilon\cos\theta)\,\mathrm{d}\theta$$

$$\simeq \frac{1}{(4\pi)^2 d}[-\pi\mathbf{H}_0(k\varepsilon)] \simeq -\frac{1}{16\pi d}\mathbf{H}_0(k\varepsilon), \quad \text{(A7)}$$

where $\mathbf{H}_0$ is the Struve function of order 0 (see reference [14] for the properties of the Struve function). Thus the correlation is

$$\mathrm{R}(k, \mathbf{x}, \mathbf{y}) \simeq \frac{1}{16\pi d}[\mathrm{J}_0(k\varepsilon) - \mathrm{i}\mathbf{H}_0(k\varepsilon)]. \quad \text{(A8)}$$

APPENDIX B: CORRELATION OF A DISCRETE LINE

The difference between the correlations of the continuous and discrete line sources is given by

$$\mathrm{R}(k,\mathbf{x},\mathbf{y})-\mathrm{R}_d(k,\mathbf{x},\mathbf{y})=\frac{1}{(4\pi)^2}\sum_{-\infty}^{+\infty}\int_{nD}^{(n+1)D}\left[\frac{\mathrm{e}^{\mathrm{i}k(r_x(l)-r_y(l))}}{r_x(l)r_y(l)}-\frac{\mathrm{e}^{\mathrm{i}k(r_x(nD)-r_y(nD))}}{r_x(nD)r_y(nD)}\right]\mathrm{d}l$$

$$=\frac{1}{(4\pi)^2}\sum_{-\infty}^{+\infty}\int_{nD}^{(n+1)D}[f(l)-f(nD)]\,\mathrm{d}l, \tag{B1}$$

where

$$f(l)=\frac{\mathrm{e}^{\mathrm{i}k(r_x(l)-r_y(l))}}{r_x(l)r_y(l)}. \tag{B2}$$

On the interval $[nD,(n+1)D]$, one has

$$\left|\int_{nD}^{(n+1)D}[f(l)-f(nD)]\,\mathrm{d}l\right|=\left|\int_{nD}^{(n+1)D}\left[\int_{nD}^{l}f'(u)\,\mathrm{d}u\right]\mathrm{d}l\right|$$

$$\leqslant\int_{nD}^{(n+1)D}\left[\int_{nD}^{l}|f'(u)|\,\mathrm{d}u\right]\mathrm{d}l\leqslant D\int_{nD}^{(n+1)D}|f'(l)|\,\mathrm{d}l. \tag{B3}$$

Therefore, one has

$$|\mathrm{R}(k,\mathbf{x},\mathbf{y})-\mathrm{R}_d(k,\mathbf{x},\mathbf{y})\leqslant\frac{D}{(4\pi)^2}\int_{-\infty}^{+\infty}|f'(l)|\,\mathrm{d}l. \tag{B4}$$

The derivative of f is given by

$$f'(l)=\left[\mathrm{i}kr'_x(l)-\mathrm{i}kr'_y(l)-\frac{r'_x(l)}{r_x(l)}-\frac{r'_y(l)}{r_y(l)}\right]f(l). \tag{B5}$$

From the result of Appendix A, one has, far from the line source,

$$r_x(l)=\sqrt{d^2+l^2}+O(1),\qquad r_y(l)=\sqrt{d^2+l^2}+O(1), \tag{B6}$$

and

$$r'_x(l)-r'_y(l)=\frac{l-x_3}{r_x(l)}-\frac{l-y_3}{r_y(l)}\simeq\frac{y_3-x_3}{\sqrt{d^2+l^2}}. \tag{B7}$$

Consequently,

$$\int_{-\infty}^{+\infty}|(r'_x(l)-r'_y(l))f(l)|\,\mathrm{d}l\leqslant|y_3-x_3|\int_{-\infty}^{+\infty}\frac{1}{(d^2+l^2)^{3/2}}\,\mathrm{d}l\leqslant\frac{2|y_3-x_3|}{d^2}. \tag{B8}$$

One also has, neglecting terms of higher order,

$$\int_{-\infty}^{+\infty}\left|\frac{r'_x(l)}{r_x(l)}f(l)\right|\mathrm{d}l\leqslant 2\int_{0}^{+\infty}\frac{l}{(d^2+l^2)^2}\,\mathrm{d}l\leqslant\frac{1}{d^2}. \tag{B9}$$

Finally, one finds that

$$|\mathrm{R}(k,\mathbf{x},\mathbf{y})-\mathrm{R}_d(k,\mathbf{x},\mathbf{y})|\leqslant\frac{2D}{(4\pi d)^2}(k|y_3-x_3|+1). \tag{B10}$$